Intramolecular energy transfer and mode-specific effects in unimolecular reactions of disilane

ARTICLE *in* THE JOURNAL OF CHEMICAL PHYSICS · JUNE 1991

Impact Factor: 2.95 · DOI: 10.1063/1.461466

3 AUTHORS, INCLUDING:

Harold W. Schranz

47 PUBLICATIONS **737** CITATIONS

SEE PROFILE

Intramolecular energy transfer and mode-specific effects in unimolecular reactions of disilane

Harold W. Schranz, Lionel M. Raff, and Donald L. Thompson
Department of Chemistry, Oklahoma State University, Stillwater, Oklahoma 74078

(Received 8 February 1991; accepted 20 March 1991)

Intramolecular energy transfer rates and pathways in disilane Si_2H_6 have been investigated in detail by analysis of the envelope functions of the time variation of the uncoupled normal-mode kinetic energies [J. Chem. Phys. **89**, 5680 (1988)] and by a new method that involves the Fourier transform of the local-mode "bond energies." The results show that the total intramolecular vibrational relaxation (IVR) rate out of a given mode is generally much faster than the total dissociation rate. However, many of the individual mode-to-mode rate coefficients are significantly smaller than this rate. Consequently, IVR is not globally rapid on the time scale of the reactions. The Si–Si and local modes relax over a much longer time scale than the Si–H modes. This observed decoupling of sets of internal modes is interpreted to mean that phase space is not explored ergodically on the time scale of the reactions, even at internal energies significantly greater than the dissociation thresholds. The present results are consistent with and complementary to our earlier observation of trajectory rate coefficients that are considerably larger than corresponding statistical phase space predictions computed on the same potential-energy surface [J. Chem. Phys. **94**, 4219 (1991)]. As a consequence, we find numerous mode-specific effects present in the system. Trajectory rates are found to be very sensitive to the nature of the initial energy partitioning. The computed kinetic isotope effects also show evidence of mode-specific chemistry. These data are consistent with the principle that a total intramolecular energy transfer rate from a given vibrational mode that is fast relative to the unimolecular reaction rate is not a sufficient condition to ensure statistical behavior and an absence of mode-specific chemistry.

I. INTRODUCTION

Recently, we reported the results of a study which showed considerable evidence for nonstatistical behavior in the unimolecular decomposition of disilane.[1] The five most important dissociation channels for this system are:

$$Si_2H_6 \rightarrow SiH_4 + SiH_2, \quad \text{(R1)}$$

$$Si_2H_6 \rightarrow SiH_3 + SiH_3, \quad \text{(R2)}$$

$$Si_2H_6 \rightarrow H_3Si\text{–}SiH + H_2, \quad \text{(R3)}$$

$$Si_2H_6 \rightarrow H_3Si\text{–}SiH_2 + H, \quad \text{(R4)}$$

$$Si_2H_6 \rightarrow H_2Si{=}SiH_2 + H_2. \quad \text{(R5)}$$

A detailed comparison of microcanonical rate coefficients for the bond fission reactions (R2) and (R4) between statistical transition state theory (EMS-TST)[1,2] and trajectory calculations[3] on the same potential-energy surface showed the presence of significant nonstatistical dynamics even at an internal energy 5.47 eV in excess of the dissociation threshold. At the lower internal energies studied, the trajectories exhibit a significantly faster rate of bond fission than the statistical theory predicts. In the case of reaction (R4), there is a switchover at higher energies after which the statistical predictions exceed the trajectory rate coefficients.

The microcanonical rate coefficient $k(E)$ can be expressed as an average over the microcanonical ensemble[4,5]

$$k(E) = \frac{1}{2}\int d\Gamma\, \delta[H(\Gamma) - E)] \times \delta(q_{RC} - q_C)|\dot{q}_{RC}| \Big/ \int d\Gamma\, \delta[H(\Gamma) - E], \quad (1)$$

where Γ is the complete set of position and momentum coordinate $[\mathbf{q},\mathbf{p}]$, $H(\Gamma)$ is the Hamiltonian of the system excluding the center-of-mass motion, $q_{RC} = q_{RC}(\mathbf{q})$ is the reaction coordinate, which may be a function of some or all of the coordinates $\mathbf{q}$, and q_C is the critical value required for reaction. The integrals in Eq. (1) are understood to be over the reactant part of phase space.

Since the critical surfaces employed in the EMS-TST calculations completely separate the reactant and product configuration space, it is impossible for Si_2H_6 to undergo either Si–Si or Si–H bond fission without traversing the critical surface. Consequently, due to trajectories that recross the critical surface, the numerator of Eq. (1) will always tend to yield upper bounds for the corresponding trajectory rates. However, as noted above, the EMS-TST results are lower than the trajectory rate coefficients at most of the internal energies investigated.[1] The only way such a result can occur is for the denominator of Eq. (1), which sums the total phase space available to the reactant system, to be larger than that which is actually available in the trajectory calculations.

 0021-9606/91/130106-15$03.00

This would mean that the trajectories are not sampling the entire phase space that is energetically accessible even though the total internal energy is well in excess of the dissociation limit where it might seem reasonable to assume that the system is ergodic. Significant nonstatistical effects are clearly present.

This behavior contrasts strongly with that obtained for the bond fission reactions of silylene (SiH_2). In this case, the EMS-TST results provide a variational upper bound to the trajectory-derived rate coefficients.[1] Viswanathan *et al.*[6] also found good agreement in a comparison of Monte Carlo transition state theory (MC-TST) and trajectory calculations for the dissociation of SiH_4 and CH_4.

The nonstatistical behavior found in Si_2H_6 indicates that, on the time scale of the reaction, intramolecular vibrational relaxation (IVR) is not complete over the entire phase space of the molecule even though it is rapid (as will be shown), relative to the unimolecular reaction rates, throughout a subset of phase space. Consequently, Si–H and Si–Si "bond energies" are observed to decay with rates significantly greater than the reaction rates. As we have previously noted,[7] the presence of such large decay rates is not a sufficient condition to guarantee the absence of nonstatistical dynamics.

It is relevant to consider the experimental systems which have been found to exhibit nonstatistical behavior. In this connection, Oref and Rabinovitch[8] noted that most thermal unimolecular reactions appear to behave statistically. Rate coefficients for such systems[8-11] are usually insensitive to the presence of nonstatistical effects and are therefore well described by statistical theories,[8] such as RRKM.[9] This insensitivity is due to the time and energy averaging inherent in experimental measurements as well as to the delocalized nature of the initial reactant state in phase space.[11,12] Exceptions to this general behavior are considered below.

A more rigorous experimental test for the presence of nonstatistical behavior is provided by methods that correspond to excitation into a relatively small part of the reactant phase space, such as chemical activation.[9,11,13-17] and state-selective laser excitation.[18-21] In these cases, quite a few experimental examples of nonstatistical behavior have been observed, although only a few have been confirmed.[15,16,17-20] In general, deviation from statistical behavior is more obvious whenever there is a local excitation and there are restrictions imposed on rapid IVR because of the molecular topology, interposing heavy masses and/or the absence of appropriate Fermi resonances. Examples include the nonrandom decomposition of chemically activated hexafluorobicyclopropyl,[15] the isomerization of allyl isocyanide,[19] and heavy mass blocking found in tetrasubstituted organometallic molecules.[16] Studies of the reaction dynamics of weakly bound complexes have yielded a great deal of evidence for and information about nonstatistical, unimolecular dynamics[22] since these systems usually have very low barriers to unimolecular dissociation and consequently the reaction rates often exceed the IVR rates.

Schlag and Levine[23] noted that lifetimes deduced from the fragmentation of large, highly excited molecules in a mass spectrometer are much shorter than statistical RRK theory would predict. They suggested that nonstatistical processes may be favorable pathways for dissociation. It has been argued[24] that there may be exceptions to statistical behavior in many-atom systems related to frequency mismatches between the molecular degrees of freedom. This may result in chemical selectivity that arises from local excitation and bond-specific energy disposal.

Heavy mass blocking of IVR on the time scale of reaction has been observed[16] for chemically activated tetrasubstituted organometallic molecules though other experiments on similar systems[17] have failed to detect such behavior. Support for the presence of heavy mass blocking of IVR has been found in a number of theoretical investigations.[11,12,25]

It has been suggested[26] that nonstatistical effects are seen in matrix-assisted uv desorption from surfaces due to the poor coupling of internal modes of the guest molecules to the lattice vibrations. Holme and Levine[27] have carried out several molecular dynamics simulations of rapid, laser-assisted desorption of a diatomic molecule from a cluster. They observed a range of dynamical behavior, ranging from statistical, with equipartitioning of energy, to highly selective where the admolecule vibration is isolated. In a recent study of S_N^2 nucleophilic substitution, Vande Linde and Hase[28] noted that collisionally formed $Cl^- \cdots CH_3Cl$ complexes exhibit unimolecular decomposition consistent with only three or fewer modes being active in IVR.

Exceptions to the generally accepted view of statistical behavior in thermal unimolecular reactions are intramolecular conversions over low barriers[29-31] and certain thermal rearrangements.[32] In a study of bond inversion in aziridine, Borchardt and Bauer[30] have observed deviations between the measured rates and RRKM predictions. They used a restricted phase-space model[30] to explain the results and suggested the presence of local bottlenecks with slow IVR on the order of 10^7–10^9 s^{-1}.[31] In a recent classical trajectory study of the nitrogen inversion in aziridine, Gai and Thompson[33] observed significant mode-specific rate enhancement. Newman-Evans *et al.*[32] obtained nonstatistical branching ratios for the thermal rearrangements of substituted bicycloalkenes and substituted cyclopropanes. The results did not seem explicable by standard statistical theories (RRKM, TST, variational TST). The authors hypothesized that the branching ratios in these reactions are largely dynamically determined and suggested that the reaction coordinate is weakly coupled to the other internal motions of the molecule; the effective number of strongly coupled internal vibrational modes is far less than the full 3N-6. It was suggested that dynamics play a large role; the favored product was the one most closely linked to the initial motions of the atoms.

Several comparisons between trajectory calculations and statistical theories show substantial disagreements.[11,12,34-38] However, most comparisons between harmonic RRKM predictions and trajectory calculations yield RRKM rates that are larger than the trajectory-derived rates by a factor of 2 up to 1.5 orders of magnitude.[34-37] As long as the statistical calculation yields upper bounds for the trajectory rates, the lack of agreement between the two cal-

culations does not necessarily demonstrate the absence of statistical behavior since the disagreement may be caused by several other factors. For example, in an early study reported by Bunker and Pattengill,[35] the standard RRKM model was replaced by a variational, anharmonic RRKM method and good agreement with trajectory calculations was obtained. Similarly, in a study of the dissociation of linear chain molecules, Schranz *et al.*[11,12] found that harmonic RRKM predictions were about a factor of 2–5 times greater than the trajectory rates but that anharmonic RRKM predictions on the same potential-energy surface were in much better accord with the trajectory data. It was also noted that, in the comparison between the trajectory and anharmonic RRKM rate coefficients, nonstatistical effects can be divided into fast dissociation at short times and slow dissociation at long times.[11,12] Similar behavior was observed by Marston and De Leon[38] in a recent model study of conformational isomerization.

In a theoretical analysis of the isomerization of *trans* stilbene in the S_1 excited state, Nordholm[39] showed how a model of limited IVR can explain the experimental observations.[40] He pointed out that a significant decrease in the reaction rate can occur even if the IVR rate is larger than the isomerization rate but still lower than the rate of decay of the isolated reactive mode (typically on the order of a vibrational frequency).

There have been many other theoretical studies of the rates and pathways of IVR for a variety of molecular models.[41–50] A number of such studies have indicated that, though extracted IVR rates are usually fast, IVR is incomplete on the time scale of the reaction.[44–49] Studies of the relaxation of local-overtone excitations produced significant evidence for mode-specific effects.[44–49] Reinhardt and Duneczky[47] have recently discussed the possibility of incomplete IVR in molecular systems. They note that there is usually rapid delocalization of an initial OH or CH excitation but the energy may remain trapped (temporary localization) within some larger moiety for a considerable period of time.[47] For example, in the OH overtone excitation of HOOH, relaxation occurs to the OOH bend in about 100 fs. However, there is no facile path for relaxation to the rest of the modes and dissociation occurs on the far longer time scale of 3 to 5 ps. They suggest that IVR in some molecules may occur as a multistage relaxation sequence.[47] Several studies by Thompson *et al.*[33,44,45] have revealed similar trends. In a study of the CH overtone excitation of methyl isocyanide, Sumpter and Thompson[45] noted that IVR occurs on several time scales: the methyl bending modes act as an energy sink for energy flow out of the excited stretches in 0.3 ps and some energy is transferred into the CNC vibrational modes on the time scale of one ps. Similar conclusions have been reached by Holme and Levine[48] in a study of high-excited acetylene. They suggested a multistep sequence of intramolecular vibrational relaxation: for short times (less than one ps), only the CH stretch motions exchange energy, at longer times, the C=C stretch exchanges energy and by about 10 ps, the bend excitation is also fully coupled. Complete relaxation takes on the order of 15 ps. In model studies of a photoinduced reaction, Rice and Gaspard[49] have observed the decoupling of slow from rapid vibrational modes. They note that Arnold diffusion (the process whereby a trajectory intersects every finite region of the energy surface in phase space for systems with more than two degrees of freedom) is sufficiently slow that there is decoupling of a part of the N-degree-of-freedom system from the rest of the system on a time scale of interest regarding subsystem internal energy transfer and chemical reaction.

In the present paper, the nonstatistical nature of the unimolecular dissociation of disilane is examined in more detail. In particular, we focus attention on the intramolecular energy transfer dynamics. Power spectral analysis of the internal coordinates from low to high energy gives some limited information on the nature of the IVR in the system. More detail is obtained by employing projection methods[7,46] to follow the relaxation of the average kinetic energy in individual normal modes. Finally, we describe a new method that, in principle, permits the complete spectrum of mode-to-mode IVR rate coefficients to be obtained from the Fourier transform of the time variation of local bond mode energies. The nonstatistical effects produced by the energy transfer dynamics are illustrated by the mode-specific chemistry seen in the results of trajectory calculations carried out using a variety of different initial states.

Although the total IVR rates in a subset of phase space are much faster than the unimolecular reaction rates, mode-specific effects are still found to be present in the bond fission reactions of disilane. We therefore conclude that global IVR is not fast and that the trajectories do not sample all of the energetically accessible phase space uniformly. This explains the failure of variational EMS-TST calculations to yield upper bounds to the trajectory rates.[1]

II. METHODS AND CALCULATIONS

A. Potential-energy surface

The potential-energy surface used in the present study is an empirical potential which has been fitted to available experimental data and to the results of *ab initio* calculations.[3] It has been previously employed in a study of Si_2H_6 unimolecular dissociation by trajectory methods[3] and by a variational transition-state procedure.[1,2] The functional form of the surface and its strengths and weaknesses are discussed at length elsewhere.[3]

B. Intramolecular energy-transfer dynamics

Our previous studies[1] show that the disilane classical trajectories do not uniformly access all of the energetically available phase space of the system. Consequently, we may anticipate that while some mode-to-mode IVR rates may be very large, the intramolecular energy transfer cannot be globally rapid. To obtain quantitative information on this point, we must have rigorous methods for monitoring the energy flow in the system and for extracting mode-to-mode rate coefficients properly averaged over the microcanonical ensemble.

One recently devised method is based upon the determination of the time dependence of the normal mode kinetic energies.[7,46] These are readily computed using the projec-

tion method previously described by Raff.[7,46] In this method, the normal-mode velocities are obtained unequivocally by projection of the Cartesian velocities onto the normal-mode vectors. Since the kinetic energy matrix is diagonal when expressed in terms of the normal-mode velocities, the mode-kinetic energies are unambiguously defined and can be computed without the omission of any coupling terms. Since the potential energy and the potential coupling terms do not enter the analysis, the method provides a classically exact description of the intramolecular energy flow in the molecule.

For the special case of an uncoupled harmonic potential, the normal-mode energies are constants of the motion. The normal-mode-kinetic energy, $K_i(t)$ for mode i, would therefore oscillate with a frequency characteristic of the mode but with an amplitude that is independent of time. The constancy of the amplitude and the zero value of the slope of the envelope function reflect the zero rate of intramolecular energy transfer. In the case of a coupled potential, the envelope function will exhibit a slope characteristic of the IVR rate.That is, if energy were rapidly leaving mode i, the amplitude of $K_i(t)$ would decrease with time and have an envelope with a negative slope whose value would reflect the IVR rate. This method has been used to extract the entire first-order mode-to-mode rate coefficient matrix for 1,2-difluoroethane.[7,46]

The average kinetic energy in mode i can be computed from

$$\langle K_i(t)\rangle = [1/\Delta t\,] \int_{t_0}^{t_0+\Delta t} ds\, K_i(s), \tag{2}$$

where t represents a time in the interval $t_0 \leqslant t \leqslant t_0 + \Delta t$. The time interval Δt can be chosen appropriately to average out most of the fluctuation in $K_i(t)$ due to the interconversion of potential and kinetic energy within the same mode. In the present calculations, we have used $\Delta t = 0.20$ ps. Ignoring residual fluctuations, the net time dependence of $\langle K_i(t)\rangle$ will reflect the rate of energy flow associated with normal mode i. For example, if energy in excess of the statistical equilibrium value $\langle K_i(\infty)\rangle$ is placed into mode i, $\langle K_i(t)\rangle$ will relax with a rate reflecting energy transfer out of the mode into all other modes to which it is effectively coupled. At long times, $\langle K_i(t)\rangle$ fluctuates about its equilibrium value.

If the relaxation process is first order, we expect

$$\langle K_i(t)\rangle = [\langle K_i(0)\rangle - \langle K_i(\infty)\rangle]e^{-\lambda_i t} + \langle K_i(\infty)\rangle, \tag{3}$$

where λ_i is the total IVR rate coefficient. In principle, λ_i is the sum of the mode-to-mode energy transfer rate coefficients connecting mode i with all of the other vibrational modes in the molecule, i.e., for disilane with 18 total vibrational modes

$$\lambda_i = \sum_{\substack{j=1 \\ (j\neq i)}}^{18} k_{ij}. \tag{4}$$

Equation (3) is based on the assumption that there is one time scale for energy relaxation out of mode i. If this is true, we may use this model to extract the total IVR rate coefficients from least-squares fits of the trajectory-derived $K_i(t)$. Since we would expect the IVR rates to depend upon the presence of resonances and the magnitude of the intermode couplings and since these quantities are functions of the distribution of energy within the molecule, a full description of the energy transfer dynamics requires that a distribution of λ_i values be computed by averaging over the microcanonical ensemble.

Although the projection method described above is exact, deconvolution of Eq. (4) to obtain the individual mode-to-mode rate coefficients k_{ij} is tedious and the uniqueness of the solution is difficult to guarantee.[7,46] We present here a new method that yields the k_{ij} values directly for a given trajectory. Appropriate distributions and average values for the k_{ij} may then be obtained in the usual manner by the integration of a group of trajectories that properly averages over the microcanonical ensemble.

Consider the computation of the time variation of a bond energy in a trajectory calculation. In the present study, we have defined such a bond energy as

$$E_B(t) = \frac{P_B(t)^2}{2\mu_B} + V_B[R_B(t)], \tag{5}$$

where the reduced mass μ_B, momentum $P_B(t)$, and bond length $R_B(t)$ are those appropriate to the bond in question and the bond potential $V_B(R_B)$, is taken to be a Morse function with parameters chosen so that it corresponds closely to the variation in potential energy on the full global surface. The reduced mass and potential parameter values for disilane are given in Table I. Most classical studies of intramolecular energy transfer have involved the calculation of some local bond energy such as that represented by Eq. (5).[33,42-45] The variation of $E_B(t)$ with time is then used to infer IVR pathways and rates.

Since Eq. (5) omits all kinetic and potential coupling terms and assumes a mode separability that does not exist, variations in the bond energy occur that are due to changes in the magnitude of the omitted coupling terms rather than to actual energy transfer between modes. The variations caused by the omitted coupling terms appear as high-frequency oscillations in the bond energy decay curve. Such oscillations are seen in every calculation that employs this approach.[33,42-45] These oscillations are directly related to the frequencies with which energy flows between the bond and the omitted coupling terms. Since it is precisely these frequencies that determine the mode-to-mode transfer rates, the entire spectrum of intermode energy transfer rate coefficients from a particular bond will be given by the Fourier transform of $E_B(t)$. The appearance of overtone and combination bands in the transform will complicate the analysis of

TABLE I. Parameters employed for the definition of local bond mode energies.

Bond	μ_B (g/mol)	D_e (eV)	r_e (Å)	β (Å^{-1})
Si–Si	14.05	3.343	2.363	1.420
Si–H	0.9404	3.131	1.479	1.629

the spectrum, but, in principle, all of the k_{ij} values can be extracted. The total rate of energy relaxation out of the relevant bond mode will then be given by Eq. (4), i.e., by summing (or integrating) over all contributions in the spectrum. By computation of appropriate averages over the microcanonical ensemble, the distribution of mode-to-mode rate coefficients can be obtained.

C. Trajectory procedures

Hamilton's equations of motion were integrated using a fourth-order Runge–Kutta routine[51] with a fixed step size of 1.018×10^{-16} s for 2.545 ps or until dissociation occurred. About four significant digits of energy conservation was generally achieved.

The unimolecular energy transfer and reaction dynamics of disilane were studied using two types of initial state sampling. The first procedure used the projection method of Raff[7,46] to insert energy into specified or randomly chosen normal modes of the molecule. With the molecule in its equilibrium configuration, zero-point vibrational energy is placed in the normal modes, and the equations of motion are integrated for a random period of time t_p,

$$t_p = \xi\tau_m, \tag{6}$$

where ξ is a random number chosen uniformly on the interval [0,1] and τ_m is the vibrational period for the lowest frequency mode in the molecule. The desired initial state is then generated by inserting the excitation energy either randomly or into specified normal modes using the projection method.[7,46]

The second method used for generating initial states of Si_2H_6 is the efficient microcanonical sampling (EMS) procedure.[52–56] This procedure has been used extensively in other studies.[1,2,11,12,52–56] Microcanonical initial states $[\mathbf{q},\mathbf{p}]$ are generated by performing a Markov walk in a reactant configuration space $\mathbf{q}$ subject to the EMS weight function

$$W(\mathbf{q}) = [E - V(\mathbf{q})]^{(3N-5)/2}, \tag{7}$$

where N is the number of atoms in the molecule. The momenta are chosen from Gaussian distributions and then scaled to reflect the correct kinetic energy, $E - V(\mathbf{q})$. The EMS procedure is discussed at length elsewhere.[52,55]

Five different types of initial states have been investigated:

(1) Miocrocanonical: The EMS algorithm[55] is used to select initial conditions.

(2) Random: Random phase-space points for total energy E are generated using projection methods.[7,46]

(3) Excited Si–H Normal Modes: After insertion of the zero-point energy, the excess excitation energy is randomly partitioned into one or all six of the Si–H stretching normal modes of Si_2H_6 using projection methods.[7,46]

(4) Excited Si–Si Normal Mode: The excess excitation energy is deposited in the Si–Si stretching normal mode.[7,46]

(5) Excited Si–H Bond Mode: The excess excitation energy is deposited into one of the six Si–H local bond modes as described by Eq. (5).

Power spectra for the internal motion of disilane were obtained from the time variation of a set of internal coordinates that include seven bond lengths, ten bond angles, and one torsional angle. A total spectrum is the sum of the area-normalized spectra obtained from the Fourier transforms of these internal coordinates. Power spectrum estimation was made using an FFT algorithm based on the routing SPCTRM described by Press *et al.*[57] The time variation of the internal coordinates were computed, beginning from specified initial states of Si_2H_6, by integration of the classical equations of motion as described above.

D. Total and individual rate coefficients

The total decay coefficient for disilane is the sum of the coefficients for all of the competing reactions (R1)–(R5),

$$k = k_1 + k_2 + k_3 + k_4 + k_5, \tag{8}$$

where k_i is the dissociation rate coefficient for reaction (Ri). If the total rate is first-order and time independent, then it must satisfy[3,9,11,12]

$$P(t) = e^{-kt}, \tag{9}$$

where $P(t)$ is the probability of undissociated reactant molecules at time t; i.e., the ratio of the number of undissociated reactant molecules at time t to the total number of trajectories computed. The rate coefficient k is obtained in this case from a least-squares fit of $P(t)$ to the model in Eq. (9).

If the decomposition process cannot be characterized by a single exponential process as suggested by Eq. (9), the rate coefficients thus extracted may still provide a meaningful, though time-averaged, description of the dissociation process. The rate coefficients for the separate reaction channels are obtained from the relative contributions of each channel to the total decomposition rate:

$$k_i = kP_{\mathrm{Ri}}(t) \Big/ \sum_{i=1}^{5} P_{\mathrm{Ri}}(t), \tag{10}$$

where $P_{\mathrm{Ri}}(t)$ is the probability of dissociation via reaction (Ri) at time t. Statistical errors are given for the 95% confidence limits[58] and are calculated using the "bootstrap" method of Efron.[59]

III. RESULTS AND DISCUSSION

A. Power spectra and IVR rates

The mode-specific effects present in the unimolecular dissociation of disilane can be related to the rate and extent of intramolecular energy flow. Some qualitative information can be gained from the power spectra of internal coordinates which are shown in Figs. 1–3. At low energy, $E = 0.18$ eV in Fig. 1, the spectral peaks are well resolved and the positions agree well with the results of a normal-mode analysis.[60] At higher energies ($E = 3.31$ eV in Fig. 2) there is some broadening and loss of structure in all of the peaks, most significantly for the six Si–H stretches located in the range 1900–2200 cm^{-1} and somewhat less for the two groups of bending deformations at 550–700 and 800–1000 cm^{-1}. At this energy, the Si–H stretches, the bending deformations and the Si–Si stretch are well isolated in frequency space. At still higher energies ($E = 5.31$ eV in Fig. 3) at which most reaction

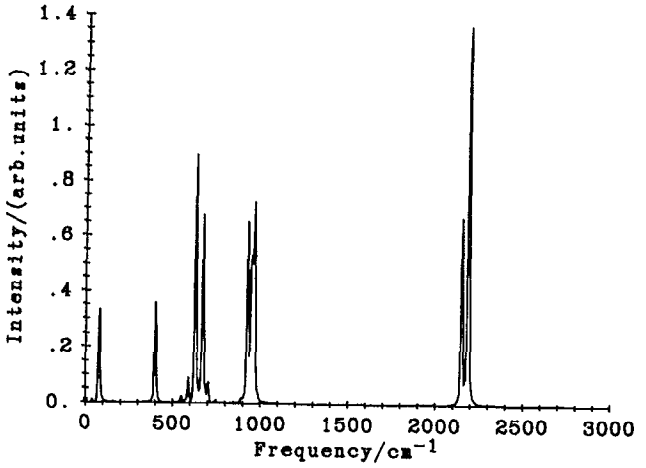

FIG. 1. Power spectra of the internal coordinates of Si_2H_6 for a randomly energized state at $E = 0.18$ eV. Obtained from a 3.13 ps trajectory using a 512 point FFT yielding a resolution of 10.7 cm^{-1}.

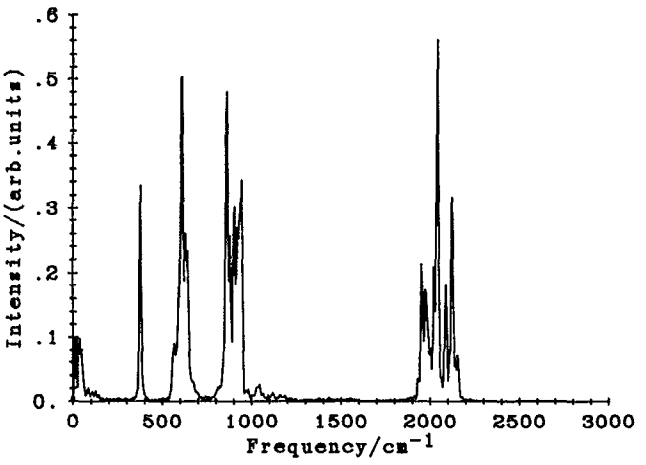

FIG. 2. Power spectra of the internal coordinates of Si_2H_6 for an excitation of the six Si–H normal modes at $E = 3.31$ eV.

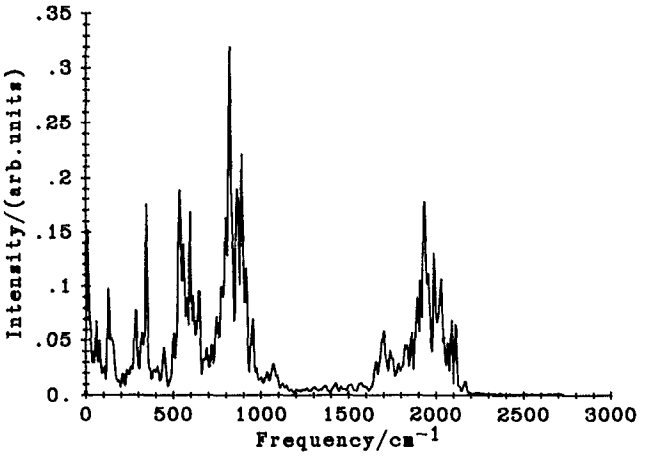

FIG. 3. Power spectra of the internal coordinates of Si_2H_6 for an excitation of the six Si–H normal modes at $E = 5.31$ eV.

channels are open, there is further broadening of the spectrum. However, a significant number of well-resolved peaks remain and the Si–H stretches are still well separated in frequency from the other modes. These spectra suggest that disilane has not reached a global chaotic threshold for IVR even at 5.31 eV. The isolated nature of the spectral peaks implies that significant regions of phase space may be isolated from each other unless some Fermi resonant energy transfer mechanism is in operation. This information is only qualitative. More detail concerning the intramolecular energy flow can be obtained by examination of the relaxation of energy in selected trajectories.

In Figs. 4 and 5, the instantaneous kinetic energy $K(t)$ is shown for the highest frequency Si–H stretch normal mode ($\nu = 2195$ cm^{-1}) and the Si–Si stretch, respectively. The initial state has a total energy of 3.31 eV; zero-point energy was inserted into all of the vibrational modes and the remaining excess energy was partitioned into either of the above Si–H or Si–Si stretching normal modes. The high-frequency oscillations reflect the transfer of kinetic energy into potential and vice versa. For the Si–H excitation, the envelope function shows that the total IVR rate corresponds to rapid relaxation on about a 0.2 ps time scale with recurrences of excess energy at later times. In contrast, the Si–Si excitation relaxes on a much longer time scale of about 3 ps. The average trend can be better seen in Figs. 6 and 7 which show the average normal-mode-kinetic energy $\langle K(t) \rangle$ obtained from Eq. (2) for the data shown in Figs. 4 and 5, respectively. A single exponential may be least-squares fitted to obtain estimates of the average decay rates. These are given in Table II for a range of initial excitations. The total IVR rates are generally on the order of 16–23 ps^{-1} for the Si–H normal mode and 9.4 ps^{-1} for the Si–Si stretch. Both of these values are greater than the dissociation rate coefficients except for local excitation at the very highest energies. We have previously found[7,46] that an overall decay rate that is fast relative to the unimolecular reaction rate is not a sufficient condition to guarantee the absence of nonstatistical,

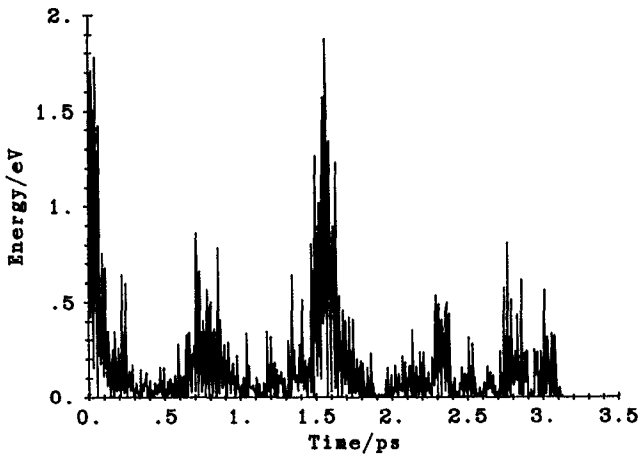

FIG. 4. Instantaneous normal-mode-kinetic energy $K(t)$ for the highest frequency Si–H stretch of the present Si_2H_6 model ($\nu = 2195$ cm^{-1}) computed from a trajectory using the projection technique of Raff (Refs. 7 and 46). The initial state involved zero-point energy in all of the vibrational modes and excitation of this normal mode to yield a total energy of $E = 3.31$ eV.

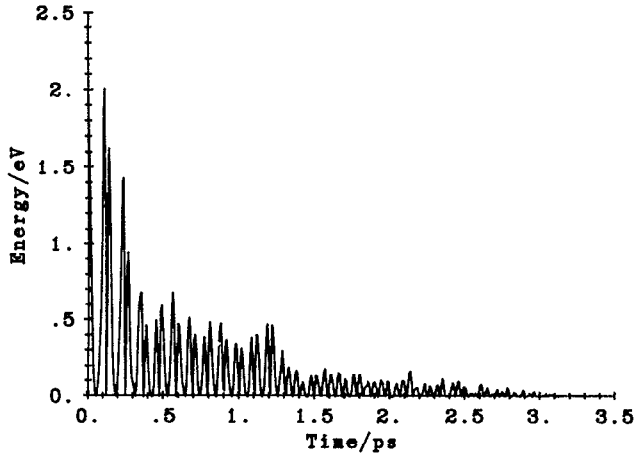

FIG. 5. As in Fig. 4 but for the Si–Si stretch ($\nu = 403\ \mathrm{cm}^{-1}$).

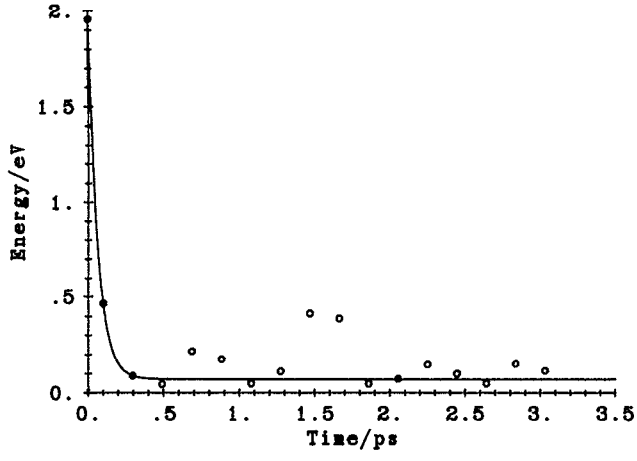

FIG. 6. Decay curve for the average normal-mode-kinetic energy of the highest frequency Si–H stretch computed from the data in Fig. 4. The solid curve is a nonlinear least-squares fit of the points to the model in Eq. (3).

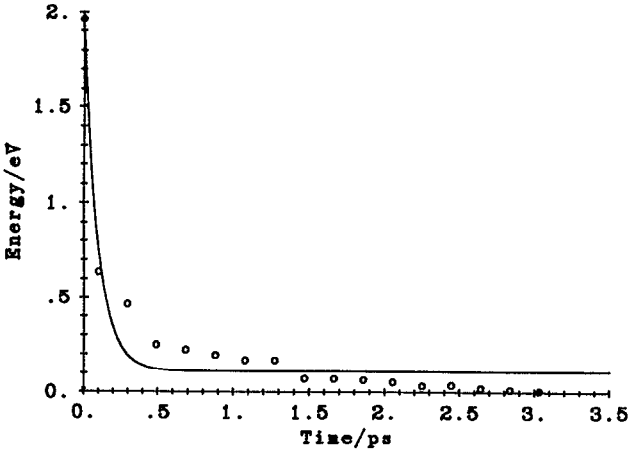

FIG. 7. Decay curve for the average normal-mode-kinetic energy of the Si–Si stretch computed from the data in Fig. 5.

TABLE II. Total IVR rates and other parameters for the single exponential model of Eq. (3) for relaxation out of specifically excited normal modes. The parameters were obtained from least-squares fits of the average normal-mode decay.

Normal mode	E(eV)	$\lambda_i\,(\mathrm{ps}^{-1})$	$\langle K(0)\rangle$(eV)	$\langle K(\infty)\rangle$(eV)
$\nu = 403\ \mathrm{cm}^{-1}$	3.31	9.4	1.92	0.08
$\nu = 2195\ \mathrm{cm}^{-1}$	3.31	16.1	1.96	0.09
$\nu = 2195\ \mathrm{cm}^{-1}$	5.31	23.0	3.96	0.12
$\nu = 2195\ \mathrm{cm}^{-1}$	6.31	21.3	4.96	0.19

mode-specific chemical effects. Disilane is clearly a case in point.

The assumption of single exponential decay may be rather simplistic as can be gauged from the quality of the fit seen in Fig. 7. A multiple exponential form would clearly be more accurate. The relaxation of Si–Si excitation seems to occur on several time scales with the fastest being of the order of $9\ \mathrm{ps}^{-1}$ but with significantly slower relaxation occurring on time scales of 1–3 ps, i.e., rates of less than $1\ \mathrm{ps}^{-1}$.

The different time scales for IVR seen in Figs. 4 and 5 indicate that relaxation is not globally rapid. Consequently, it is not surprising that nonstatistical and mode-specific effects are present in the unimolecular dissociation of disilane.[1]

We may extract the mode-to-mode rate coefficients as well as additional information related to the intramolecular energy flow by examining the time dependence of the local bond mode energies. Figure 8 shows $E_B(t)$ for the six Si–H and the Si–Si bonds over the range $0 \leqslant t \leqslant 25$ ps for one disilane trajectory ($E = 3.31$ eV) with zero-point energy in all normal modes and the excess energy partitioned into the highest frequency Si–H stretching normal mode. Clearly, rapid energy exchange between the six Si–H bond modes is occurring on a subpicosecond time scale. On the other hand, there is no significant energy flow into the Si–Si bond mode

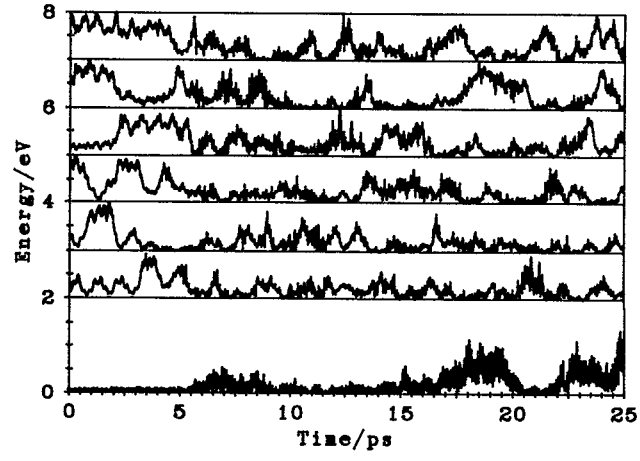

FIG. 8. Local-bond mode energies for Si_2H_6. The initial state involved zero-point energy in all of the vibrational modes and excitation of the highest frequency Si–H normal mode to yield a total energy of $E = 3.31$ eV. The lowest curve is for the Si–Si bond-mode energy and higher curves are for the six Si–H bond-mode energies. Each successive curve has been displaced upwards by 1.0 eV to provide visual clarity.

for times less than 2 ps and very little for times less than 5 ps. Similar behavior is observed even if the excess energy is partitioned into all six Si–H normal modes as shown in Fig. 12. of Ref. 1.

When the initial state corresponds to a local excitation of an Si–H bond mode, the relaxation rate is much slower than is the case for normal-mode excitation. Figure 9 shows the decay of $E_B(t)$ for an initial state corresponding to zero-point energy in all normal modes with the excess energy present as local-mode excitation in one of the Si–H bond modes to yield a total internal energy of 3.31 eV. Comparison of this result with the data shown in Fig. 4 and 8 clearly demonstrates that the Si–H local-mode relaxation rate is much slower than that for the Si–H normal modes. The result of averaging the local-mode decay curves for 20 trajectories is shown in Fig. 10. the average local-mode decay is nearly exponential

$$E_B(t) = [E_B(0) - E_B(\infty)]e^{-\lambda_i t} + E_B(\infty). \quad (11)$$

A least-squares fit of Eq. (11) to the data in Fig. 10 yields a total average decay rate coefficient λ_i of 0.48 ps^{-1}. Further rate constants for average local-mode decay for different initial energies and energization patterns are given in Table III.

The local-mode energies defined by Eq. (5) exhibit the high-frequency oscillations characteristic of such quantities.[33,42–45] The data shown in Figs. 8 and 9 are therefore typical. The corresponding oscillations seen in Fig. 10 are significantly reduced due to the randomness of the phases which causes the oscillations to cancel when 20 trajectories are averaged. It has been pointed out in Sec. II that these fluctuations are due to energy flow in and out of the kinetic and potential coupling terms that are omitted from the definition of $E_B(t)$. Since the rate of energy flow between vibrational modes depends upon the rate of flow into the coupling terms, the spectrum of mode-to-mode IVR rate coefficients out of a given local mode can be obtained from the Fourier transform of $E_B(t)$.

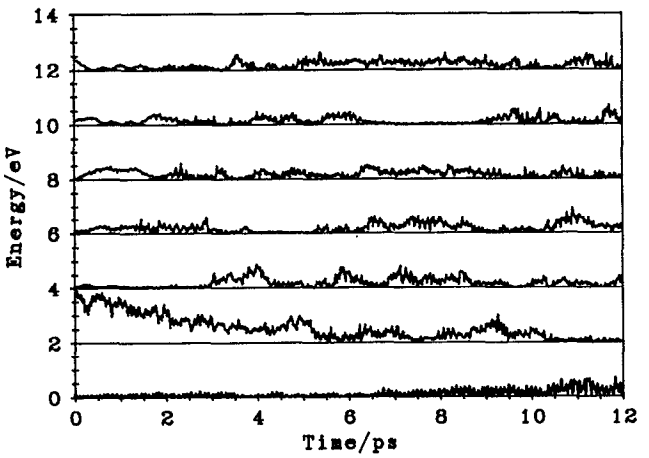

FIG. 9. As in Fig. 8 but for an initial state involving zero-point energy in all of the normal modes and excitation of a Si–H local bond mode to yield a total energy of $E = 3.31$ eV. Each successive curve has been displaced upwards by 2.0 eV to provide visual clarity. The excited mode corresponds to the curve next to the bottom. The lowest frame is the Si–Si local bond energy.

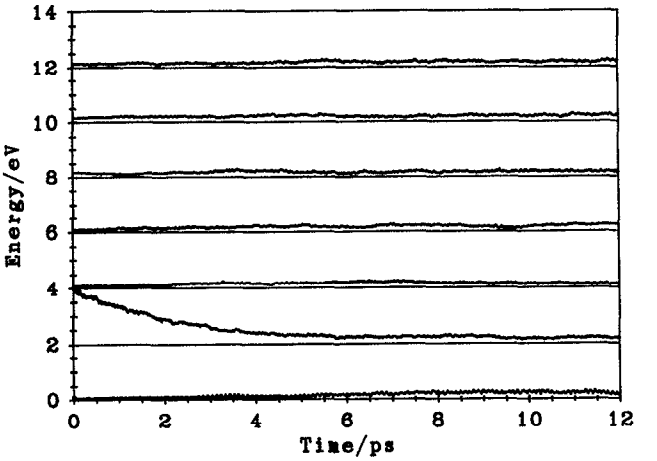

FIG. 10. As in Fig. 9, but averaged over the results of 20 trajectories each of which initially has zero-point energy in all of the normal modes and excitation of the same Si–H local bond mode to yield a total energy of 3.31 eV.

We have obtained the Fourier transforms of $E_B(t)$ for each of the 20 trajectories that yield the results given in Fig. 10. The ensemble average of these 20 spectra is shown in Fig. 11. The result is a series of relatively broad peaks spanning the range 0.0–0.4 ps^{-1} that represent the average mode-to-mode rate coefficients for Si–H local-mode relaxation to the other 17 modes in disilane along with the overtone and combination bands. Equation (4) indicates that the average mode-to-mode rate coefficient $\langle k_{ij} \rangle$ should be given by

$$\langle k_{ij} \rangle = \lambda_i / 17. \quad (12)$$

The least-squares fit of the average decay curve in Fig. 10 yields $\lambda_i = 0.48$ ps^{-1} so that we would expect to find $\langle k_{ij} \rangle = 0.028$ ps^{-1}. The spectrum in Fig. 11 is clearly consistent with this expectation. The major components of the spectrum are broad peaks centered at 0.04 and 0.16 ps^{-1}. The limited spectral resolution (0.08 ps^{-1}) precludes the determination of the individual k_{ij}. However, this problem could, in principle, be overcome by integration of the trajectories for much longer periods. We interpret the low-intensity, higher frequency bands that appear in Fig. 11 to be overtones and combination bands of the k_{ij}.

B. Nonstatistical and mode-specific effects

Our previous EMS-TST and trajectory calculations[1–3] have demonstrated the existence of nonstatistical behavior in the unimolecular dissociation dynamics of disilane. The above IVR results show that the total decay rates for individ-

TABLE III. Total IVR rates for energy transfer out of a local bond mode. These were estimated from least-squares fits of Eq. (11) to the local bond mode decay averaged over ensembles of 20 trajectories.

Excited mode	E(eV)	λ_i (ps^{-1})	$E_B(0)$(eV)	$E_B(\infty)$(eV)
Si–H bond mode	3.31	0.48	1.99	0.16
Si–H bond mode	4.31	1.48	2.90	0.27
Si–Si normal mode	3.31	0.80	1.86	0.35

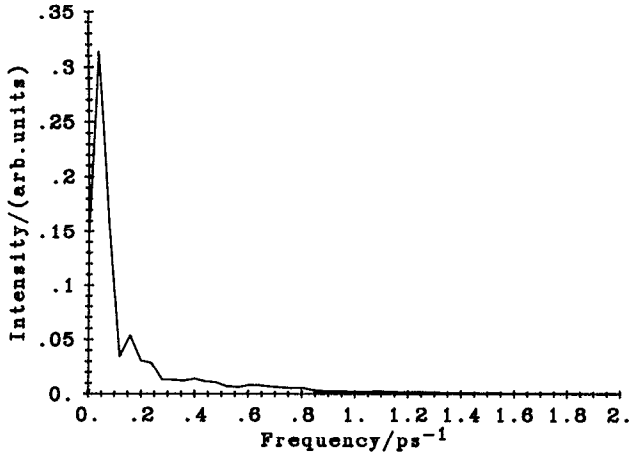

FIG. 11. Ensemble average of the 20 spectra obtained from the Fourier transforms of $E_B(t)$ for each of the 20 trajectories used to obtain the average decay curve for Si–H local bond mode excitation at 3.31 eV shown in Fig. 10 as the curve next to the bottom. The spectral resolution is 0.08 ps^{-1}.

ual vibrational modes are large relative to the unimolecular reaction rates.[1,3] However, IVR is not globally rapid. Consequently, the trajectories do not explore all of the energetically accessible phase space on the time scale of unimolecular dissociation. This leads to nonstatistical behavior and, we may anticipate, mode-specific effects.

We have investigated the system for the presence of such mode-specific effects by running batches of 250 classical trajectories at total energies ranging from 5.31 to 9.31 eV employing the first four of the five different initial energization patterns described in Sec. II: microcanonical, random, Si–H, and Si–Si normal mode excitations.

Figure 12 shows a decay plot for the reactant probability $P(t)$ for microcanonical energization of Si_2H_6 at 6.31 eV. The points are obtained from the trajectory lifetime data and the line is a least-squares fit of the single exponential model, Eq. (9). The slope of the line yields a total decay coefficient of 0.289 ± 0.047 ps^{-1}. This value is substantially less than the total energy relaxation rates discussed above, but *it is significantly greater than many of the individual mode-to-mode rate coefficients that appear in the frequency spectra in Fig. 11.* This type of behavior is typical of that found at the lower energies, 5.31 to 7.31 eV, for microcanonically and randomly initialized trajectories. The decay is well described by the single exponential model of Eq. (9). Since our previous calculations[1] and the present IVR results show that energy transfer is not globally rapid and that the system does not behave statistically, it is clear that the observation of an exponential decay, such as seen in Fig. 12, is not sufficient to guarantee statistical behavior. That is, if a system is known to be statistical, the decay will be exponential, but the reverse is not true.

Figure 13 shows the decay plot obtained for energization of the six Si–H normal modes of Si_2H_6 at 6.31 eV. If IVR were globally rapid, we would expect this result to be nearly identical to that obtained upon microcanonical initialization at this energy. Comparison of these data with those shown in Fig. 12 demonstrates that such is not the case. Mode-specific chemistry is clearly present. Excitation of the Si–H modes results in unimolecular decomposition that is not well described by a single exponential model such as Eq. (9). Initially ($t \leqslant 0.1$ ps), there is a very fast decay followed by a much slower decomposition for $t \geqslant 0.1$ ps. Each of these regions is well described by Eq. (9) but with different rate coefficients. Separate least-squares fits of the two time ranges yield rate coefficients of 7.66 and 0.392 ps^{-1}, respectively. Both of these values are substantially larger than the result obtained by microcanonical initialization with $E = 6.31$ eV. Consequently, the mode-specific, nonstatistical nature of the dynamics is obvious.

At internal energies above 8.30 eV, the dissociation dynamics cannot be accurately fitted by a single exponential expression such as Eq. (9) regardless of the nature of the initialization method. Figures 14 and 15 provide typical examples. These figures show decay plots for microcanonical initialization at energies of 8.31 and 9.31 eV, respectively.

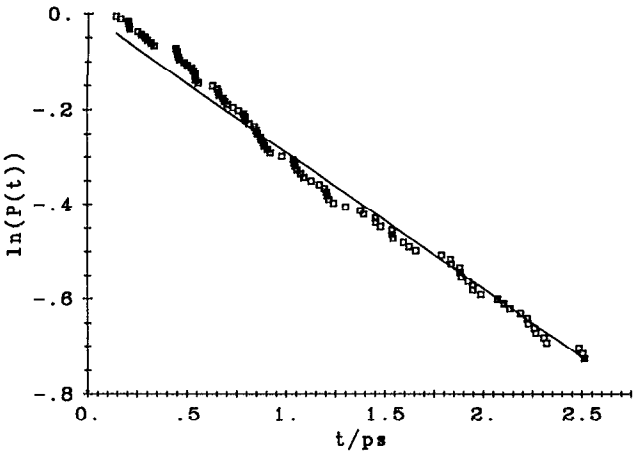

FIG. 12. Decay of reactant probability $P(t)$ for microcanonical energization of Si_2H_6 at $E = 6.31$ eV. Points are from trajectory lifetime data and line is the nonlinear least squares fit of the single exponential model, Eq. (9).

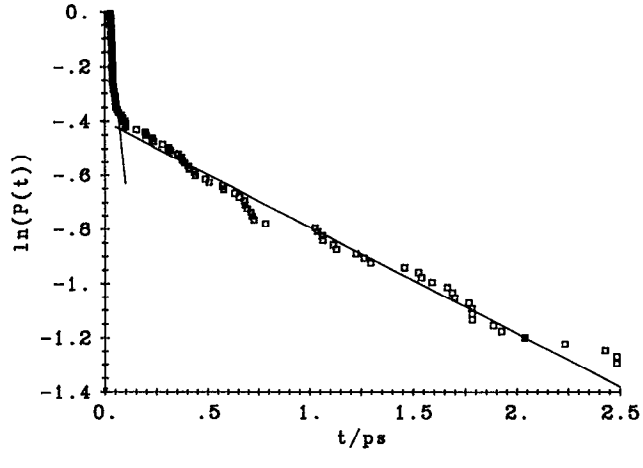

FIG. 13. Decay of reactant probability $P(t)$ for local energization of the six Si–H normal modes of Si_2H_6 at $E = 6.31$ eV. Points are from trajectory lifetime data and the two lines represent separate nonlinear least squares fit of the single exponential model $P(t) = Ae^{-kt}$ for times $t < 0.1$ ps ($k = 7.66$ ps^{-1}) and times $t > 0.1$ ps ($k = 0.392$ ps^{-1}).

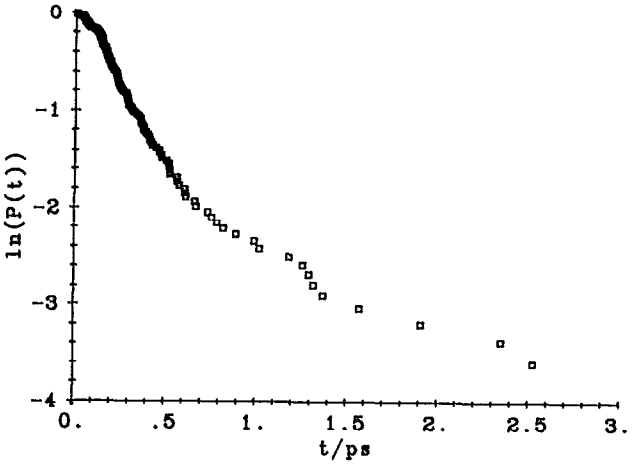

FIG. 14. Decay of reactant probability $P(t)$ for microcanonical energization of Si_2H_6 at $E = 8.31$ eV.

The nonexponential character of the results is evident. Usually, these plots contain two major components: a dominant set of fast dissociations at short times (< 0.7 ps) and a smaller set of slow dissociations at longer times. Consequently, we would expect a significantly better fit to result from the use of a biexponential function. A more accurate fit would consider $P(t)$ or the related lifetime distribution $h(t)$,[11,12]

$$h(t) = -[dP(t)/dt], \tag{13}$$

in its entirety. More detail on the dissociation process could be obtained from an examination of the time-dependent rate coefficient

$$k(t) = -h(t)/P(t)$$
$$= h(t)\left[P(t=0) - \int_0^t ds\, h(s)\right]^{-1}, \tag{14}$$

as has been done by Schranz *et al.*[11,12] in a study of linear chain systems. However, since our objective here is to demonstrate the presence and extent of mode-specific effects, we shall content ourselves with simple least-squares fits of Eq. (9) to the trajectory data. If the decay is nonexponential or multiexponential in character, then the results of such a fit will be an average of the different time scales inherent in the decay. Since the value so obtained will be dependent upon the fitting procedure and the time domain over which the fit is made, we will employ identical methods and time domains for all fits. The essential point is that if there are no mode-specific effects present, then the average rate coefficients obtained in the above manner will be nearly identical for the same internal energy regardless of the method used for initialization.

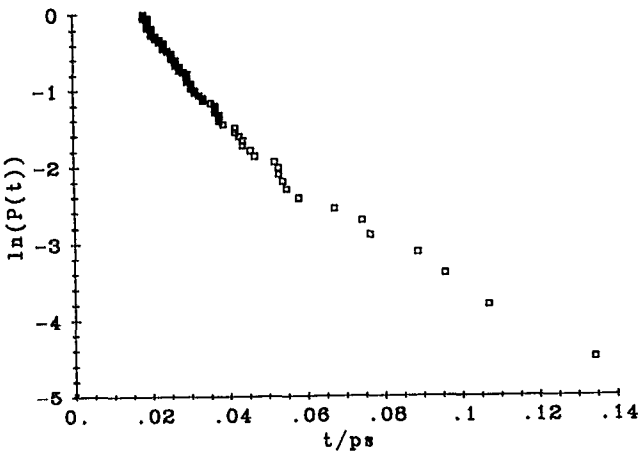

FIG. 15. Decay of reactant probability $P(t)$ for local energization of the six Si–H normal modes of Si_2H_6 at $E = 9.31$ eV.

The total and individual average unimolecular rate coefficients obtained from the trajectory lifetime data using Eqs. (9) and (10) are given in Table IV and Fig. 16. Despite the inherent averaging introduced by the fitting process, it is clear that the total unimolecular rate coefficients are very sensitive to the method used for initialization. The microcanonically energized ensembles have the slowest rate coefficients. The randomly prepared ensembles yield dissociation coefficients that are similar, but systematically larger. The most significant mode enhancement of the total decay rate is found for the ensembles involving excitation of the Si–H stretches or excitation of the Si–Si stretch.

The individual rate coefficients for channels (R1)–(R4) are even more sensitive to the nature of the initialization. For example, although the microcanonical and random energization patterns yield similar individual rate coefficients at the lower energies, there are significant differences at higher energies. At $E = 9.31$ eV, there is more dissociation via the $SiH_3 + SiH_3$ channel for microcanonical than for random energization. Apparently, there is less time for IVR to occur to equalize the delocalization of the two ensembles in phase space. The more localized ensembles involving energization into the Si–H or the Si–Si stretch exhibit significant mode-specific enhancement for decomposition pathways involving Si–H or Si–Si bond cleavage, respectively. This is particularly true at the highest energy studied, $E = 9.31$ eV. In the case of Si–H stretch excitation, the reaction rate decreases with internal energy allowing more time for IVR to occur. Thus we observe less mode specificity at the lower energies ($E = 6.31$, 7.31 eV) and a significant amount of reaction involving Si–Si bond cleavage.

Figures 17 and 18 show a comparison of the trajectory-computed rates for Si–Si and Si–H bond fission, respectively, using the four different initialization methods. These figures also show the trajectory results previously reported by Agrawal *et al.*[3] and the predictions of variational transition-state theory based on EMS sampling (EMS-TST).[1] As we have described in our previous work,[1] the statistical predictions shown by the open circles and dotted RRK fit are generally lower than the rate coefficients calculated from trajectories with the initial states generated using the EMS energization pattern. This deviation is greater for Si–Si bond fission than for Si–H bond cleavage. In the latter case at higher energies, the EMS-TST results undergo a switchover and exceed the trajectory results with EMS sampling and the random sampling of Agrawal *et al.*,[3] but still give slightly slower rates than the present random sampling calculations. In the case of Si–Si bond fission, most of the trajectory rates are far larger than the EMS-TST predictions.

TABLE IV. Individual and total microcanonical rate constants for the decomposition of Si_2H_6 initially excited with different energization patterns. Rate constants are determined from the trajectory lifetime data as described in Sec. II.

	$k(E)(ps^{-1})$				
E(eV)	$SiH_2 + SiH_4$	$SiH_3 + SiH_3$	$H_3SiSiH + H_2$	$Si_2H_5 + H$	Total
(a) Microcanonical energization					
5.31	0.029 ± 0.012	0.008 ± 0.006	0.006 ± 0.006	0.000 ± 0.000	0.043 ± 0.015
6.31	0.114 ± 0.029	0.114 ± 0.028	0.060 ± 0.021	0.000 ± 0.000	0.289 ± 0.047
7.31	0.208 ± 0.063	0.587 ± 0.119	0.312 ± 0.081	0.052 ± 0.030	1.16 ± 0.192
8.31	0.193 ± 0.104	1.68 ± 0.32	0.406 ± 0.152	0.463 ± 0.174	2.74 ± 0.48
9.31	0.068 ± 0.074	4.17 ± 0.59	0.410 ± 0.197	0.342 ± 0.184	4.99 ± 0.67
(b) Random energization					
5.31	0.036 ± 0.013	0.007 ± 0.006	0.021 ± 0.010	0.000 ± 0.000	0.064 ± 0.017
6.31	0.138 ± 0.031	0.071 ± 0.021	0.192 ± 0.038	0.013 ± 0.009	0.414 ± 0.057
7.31	0.221 ± 0.069	0.418 ± 0.094	0.650 ± 0.141	0.232 ± 0.082	1.52 ± 0.23
8.31	0.208 ± 0.120	1.20 ± 0.27	1.17 ± 0.360	0.781 ± 0.291	3.36 ± 0.67
9.31	0.358 ± 0.232	2.21 ± 0.39	1.37 ± 0.48	2.57 ± 0.75	6.50 ± 0.82
(c) Local energization into Si–H stretches					
5.31	0.012 ± 0.006	0.006 ± 0.004	0.048 ± 0.017	0.091 ± 0.027	0.157 ± 0.038
6.31	0.052 ± 0.019	0.043 ± 0.019	0.337 ± 0.077	0.484 ± 0.101	0.915 ± 0.157
7.31	0.103 ± 0.288	0.207 ± 0.443	1.55 ± 1.32	8.58 ± 3.73	10.4 ± 4.1
8.31	0.000 ± 0.000	0.184 ± 0.355	0.920 ± 0.926	16.4 ± 3.0	17.5 ± 3.1
9.31	0.000 ± 0.000	0.000 ± 0.000	0.000 ± 0.000	23.3 ± 2.4	23.3 ± 2.4
(d) Local energization into Si–Si stretch					
5.31	0.000 ± 0.000	4.73 ± 0.24	0.000 ± 0.000	0.000 ± 0.000	4.73 ± 0.24
6.31	0.026 ± 0.037	6.37 ± 0.026	0.000 ± 0.000	0.000 ± 0.000	6.39 ± 0.25
7.31	0.000 ± 0.000	7.46 ± 0.31	0.000 ± 0.000	0.000 ± 0.000	7.46 ± 0.31
8.31	0.000 ± 0.000	8.34 ± 0.36	0.000 ± 0.000	0.000 ± 0.000	8.34 ± 0.36
9.31	0.000 ± 0.000	9.15 ± 0.40	0.000 ± 0.000	0.000 ± 0.000	9.15 ± 0.40

As discussed in Sec. I and elsewhere,[1] such results can only be obtained in systems that exhibit nonstatistical intramolecular energy flow, i.e., in systems in which dynamical consideration play a major role in determining product formation. The only way the statistical calculations can fail to produce upper bounds for the trajectory rates is for the total energetically available phase space to be larger than that which is actually explored by the trajectories. We have therefore concluded that the disilane trajectories sample only a subset of the available phase space even though the total internal energies are well above the dissociation thresholds for Si–H and Si–Si bond fission.[1]

Figures 19 and 20 show the corresponding results for the $SiH_2 + SiH_4$ and $H_3SiSiH + H_2$ dissociation channels,

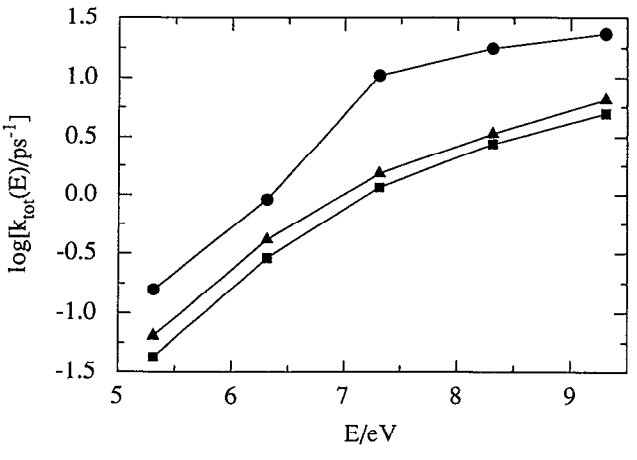

FIG. 16. Total microcanonical rate constants for the decomposition of Si_2H_6 initially excited with different energization patterns: Filled squares (■), microcanonical; filled triangles (▲), random; filled circles (●), Si–H stretches. Rate constants are determined from the trajectory lifetime data as described in Sec. II.

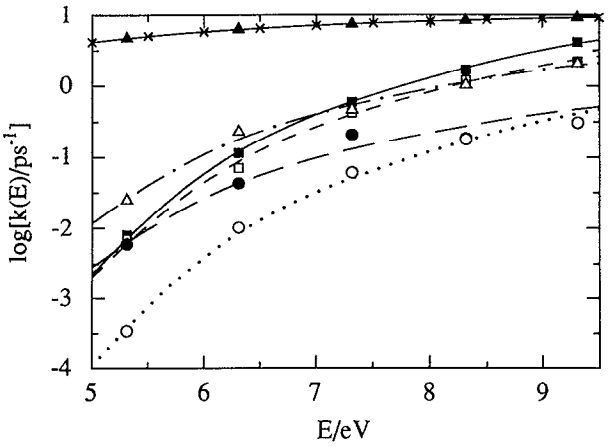

FIG. 17. Comparison of microcanonical rate constants for $Si_2H_6 \rightarrow SiH_3 + SiH_3$: In this figure and Figs. 18–20, calculated points are denoted by symbols and corresponding RRK fits by smooth curves: Filled squares (■) and solid line (—), microcanonical; open squares (□) and short-dashed line (- - -), random; filled circles (●) and long-dashed line (— — —), Si–H stretches; open circles (○) and dotted line (· · ·), EMS-TST predictions (Ref. 1); open triangles (△) and dot–dash line (-·-), Agrawal *et al.* (Ref. 3) filled triangles (▲) and crossed-solid line (-×-), Si–Si stretch. Trajectory rate constants from this work are determined from the lifetime data as described in Sec. II.

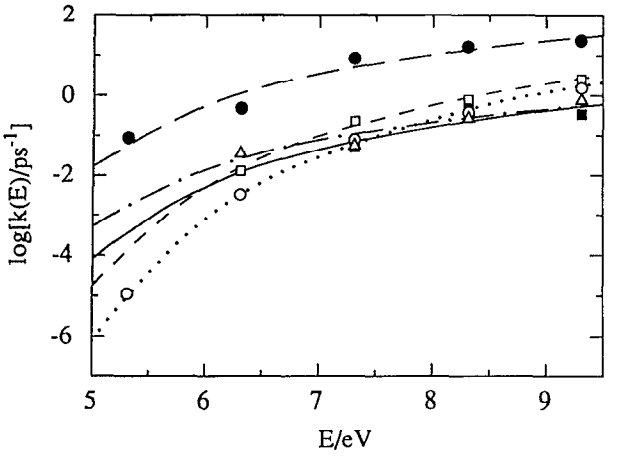

FIG. 18. Comparison of microcanonical rate constants for $Si_2H_6 \rightarrow Si_2H_5 + H$. Symbols as for Fig. 17.

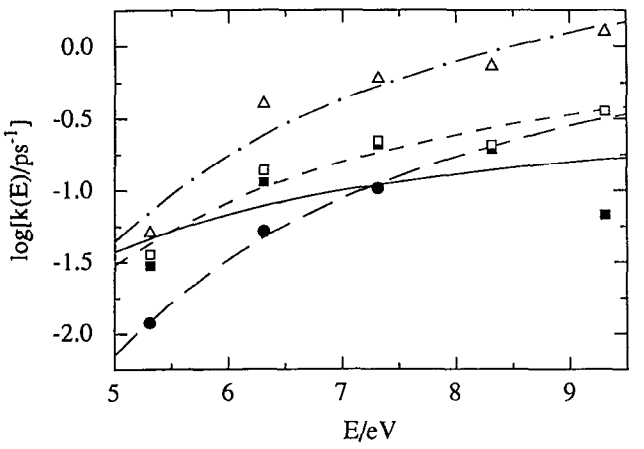

FIG. 19. Comparison of microcanonical rate constants for $Si_2H_6 \rightarrow SiH_2 + SiH_4$. Symbol identification as for Fig. 17.

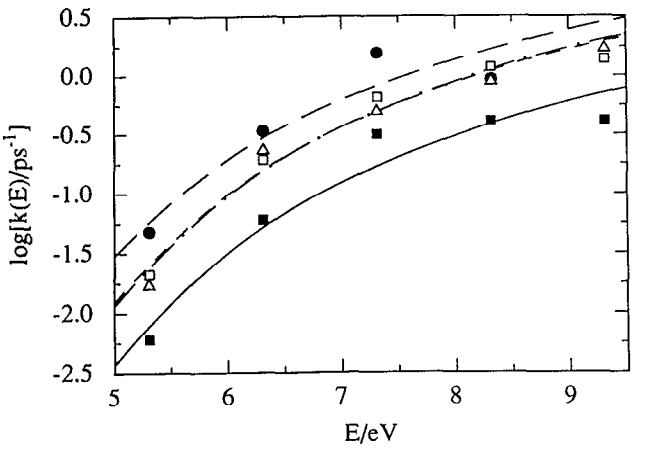

FIG. 20. Comparison of microcanonical rate constants for $Si_2H_6 \rightarrow H_3SiSiH + H_2$. Symbol identification as for Fig. 17.

respectively, reactions (R1) and (R3). Statistical calculations were not carried out for these multicentered reactions. We note that the reaction rate coefficients for all channels are very sensitive to the mode of initialization. Consequently, we see mode-specific effects for channels (R1)–(R4). We have been unable to obtain sufficient data on reaction (R5) due to its very low probability to permit reliable conclusions to be drawn. Our previous trajectory data, which is shown in Figs. 17–20 as open triangles and dot–dash RRK fits, utilize a random mode of initialization. They should therefore agree with the present data shown as open squares and short-dashed RRK fits in Figs. 17–20. Reasonable agreement is seen for all channels except (R1) (Fig. 19). Part of the discrepancy may be due to the relatively small batch size run in the earlier work (100–200) and even in the present calculations (250). However, the presence of mode-specific effects means that rigorous constraints on the sampling methods for covering phase space are present. Even slight differences in initial conditions can lead to very different rate coefficients.

C. Isotope effects

We have computed microcanonical reaction rate coefficients using different initialization methods for Si_2D_6. These results are given in Table V. Comparison with the data in Table IV shows Si_2D_6 to be qualitatively similar to Si_2H_6. These rate coefficients have been fitted to an RRK form

$$k(E) = \nu[(E - E_0)/E]^{s-1}, \tag{15}$$

with E_0 taken to be the barrier height for reaction. The resulting RRK parameters along with the least-squares regression coefficient r are given in Tables VI and VII for Si_2H_6 and Si_2D_6, respectively. The RRK fits are also shown as curves in Figs. 17–20.

The effect of deuteration on the total and individual rate coefficients is small. This is, in large measure, due to the relatively high total energies considered. In addition, the static quantum effect due to the change in zero-point energy is absent in the present calculations because the trajectories invoke only classical mechanics. The greatest effect is predicted to be for reactions involving the substituted atoms, i.e., the channels involving Si–H (Si–D) bond dissociation. The channels involving Si–Si bond cleavage, reactions (R1) and (R2), have $k_D(E)/k_H(E)$ ratios closer to unity whereas channels (R3) and (R4) tend to have smaller values for this ratio. These data are given in Table VIII. There is some additional evidence of nonstatistical behavior in that the $k_D(E)/k_H(E)$ ratio is sometimes greater than unity.

IV. CONCLUSIONS

Intramolecular energy transfer rates and pathways in disilane have been investigated in detail. It is found that although the total relaxation rates out of the various vibrational modes are large relative to the unimolecular reaction rates, the relaxation is not globally rapid. This leads to the nonstatistical behavior we have previously reported[1] for this system and to the mode-specific effects that we report in this paper.

IVR rates and pathways have been obtained by analysis of the envelope functions of the time variation of the uncou-

TABLE V. Individual and total microcanonical rate constants for the decomposition of Si_2D_6 initially excited with different energization patterns. Rate constants are determined from the trajectory lifetime data as described in Sec. II.

	$k(E)(ps^{-1})$				
E(eV)	$SiD_2 + SiD_4$	$SiD_3 + SiD_3$	$D_3SiSiD + D_2$	$Si_2D_5 + D$	Total
(a) Microcanonical energization					
5.31	0.023 ± 0.010	0.008 ± 0.006	0.007 ± 0.005	0.000 ± 0.000	0.038 ± 0.013
6.31	0.087 ± 0.022	0.096 ± 0.024	0.029 ± 0.013	0.002 ± 0.003	0.214 ± 0.037
7.31	0.200 ± 0.047	0.365 ± 0.069	0.185 ± 0.047	0.005 ± 0.006	0.756 ± 0.110
8.31	0.242 ± 0.098	1.33 ± 0.25	0.257 ± 0.102	0.303 ± 0.124	2.14 ± 0.37
9.31	0.168 ± 0.102	3.32 ± 0.50	0.391 ± 0.151	0.140 ± 0.098	4.02 ± 0.52
(b) Random energization					
5.31	0.025 ± 0.010	0.007 ± 0.005	0.015 ± 0.008	0.000 ± 0.000	0.047 ± 0.014
6.31	0.102 ± 0.026	0.108 ± 0.027	0.128 ± 0.032	0.007 ± 0.006	0.344 ± 0.054
7.31	0.244 ± 0.080	0.478 ± 0.120	0.616 ± 0.154	0.085 ± 0.050	1.42 ± 0.27
8.31	0.224 ± 0.112	1.16 ± 0.28	0.611 ± 0.208	0.407 ± 0.182	2.40 ± 0.46
9.31	0.113 ± 0.113	2.00 ± 0.33	0.716 ± 0.281	1.39 ± 0.46	4.22 ± 0.56
(c) Local energization into Si–D stretches					
5.31	0.018 ± 0.008	0.000 ± 0.000	0.040 ± 0.015	0.089 ± 0.027	0.147 ± 0.035
6.31	0.092 ± 0.026	0.046 ± 0.022	0.231 ± 0.056	0.600 ± 0.126	0.969 ± 0.164
7.31	0.092 ± 0.202	0.275 ± 0.419	0.916 ± 0.738	7.97 ± 2.13	9.25 ± 2.25
8.31	0.000 ± 0.000	0.000 ± 0.000	0.433 ± 0.503	13.6 ± 1.6	14.0 ± 1.5
9.31	0.000 ± 0.000	0.000 ± 0.000	0.183 ± 0.283	17.0 ± 1.5	17.2 ± 1.4
(d) Local energization into Si–Si stretch					
5.31	0.446 ± 0.317	2.53 ± 1.28	0.000 ± 0.000	0.000 ± 0.000	2.97 ± 1.40
6.31	0.219 ± 0.132	4.07 ± 0.77	0.040 ± 0.055	0.000 ± 0.000	4.34 ± 0.79
7.31	0.023 ± 0.033	5.49 ± 0.56	0.000 ± 0.000	0.000 ± 0.000	5.52 ± 0.56
8.31	0.025 ± 0.036	6.31 ± 0.57	0.000 ± 0.000	0.000 ± 0.000	6.34 ± 0.56
9.31	0.000 ± 0.000	7.38 ± 0.55	0.000 ± 0.000	0.000 ± 0.000	7.38 ± 0.55

pled normal-mode-kinetic energies[7,46] and by a new method that involves the Fourier transform of the local mode bond energies $E_B(t)$. This transform yields a frequency spectrum that contains the mode-to-mode rate coefficients for energy transfer out of the mode in question. The results show that the total IVR rate out of a given mode is generally much faster than the total dissociation rate. However, many of the individual mode-to-mode rate coefficients obtained from the Fourier transform of $E_B(t)$ are significantly smaller than this rate. Consequently, intramolecular relaxation is not globally rapid on the time scale of the reactions. The Si–Si normal and local modes relax over a much longer time scale than the Si–H modes. Over a time scale of about 5 ps, the Si–Si modes are decoupled from the rapid intramolecular ener-

TABLE VI. RRK parameters (E_0,ν,s) and correlation coefficient r for RRK fits to the Si_2H_6 dissociation rate constants for each channel. Rate constants are obtained from current trajectory calculations, those of Agrawal *et al.* (Ref. 3) and EMS-TST calculations (Ref. 1).

Channel	Calculation	E_0(eV)	$\nu(ps^{-1})$	s	r
$SiH_4 + SiH_2$	EMS	2.46	0.552	4.96	0.607
	Random		2.86	7.72	0.962
	Si–H modes		7.37	11.3	0.996
	Agrawal		23.7	10.27	0.964
$SiH_3 + SiH_3$	EMS	3.29	651	12.7	1.000
	Random		291	12.1	0.999
	Si–H modes		15.5	9.02	0.976
	Si–Si mode		15.6	2.23	1.000
	Agrawal		49.9	8.52	0.982
	EMS-TST		117	14.0	0.997
$H_3SiSiH + H_2$	EMS	2.61	48.3	13.8	0.969
	Random		115	13.4	0.987
	Si–H modes		108	12.1	0.939
	Agrawal		130.5	13.7	0.981
$Si_2H_5 + H$	EMS	3.84	77.4	10.4	0.851
	Random		2485	13.8	0.996
	Si–H modes		1901	8.96	0.977
	Agrawal		21.4	8.03	0.967
	EMS-TST		7489	16.7	0.999

TABLE VII. RRK parameters (E_0, ν, s) and correlation coefficient r for RRK fits to the Si_2D_6 dissocation rate constants for each channel. Rate constants obtained as in Table VI.

Channel	Calculation	E_0 (eV)	ν (ps^{-1})	s	r
$SiD_4 + SiD_2$	EMS	2.46	2.41	8.06	0.923
	Random		1.39	6.82	0.797
	Si-D modes		3.32	9.11	0.918
$SiD_3 + SiD_3$	EMS	3.29	375	12.2	0.998
	Random		257	11.8	0.998
	Si-D modes		605	13.9	1.000
	Si-Si mode		17.1	2.94	0.997
$D_3SiSiD + D_2$	EMS	2.61	25.4	13.2	0.986
	Random		51.6	12.6	0.962
	Si-D modes		3.27	6.61	0.665
$Si_2D_5 + D$	EMS	3.84	181	13.5	0.895
	Random		1321	14.0	1.000
	Si-D modes		1234	8.53	0.982

gy flow involving the Si–H modes. Excited Si–H local modes relax at a slower rate than excited Si–H normal modes.

The present results are consistent with the previously stated principle[7,46] that a total intramolecular energy transfer rate that is fast relative to the unimolecular reaction rate is not a sufficient condition to ensure statistical behavior and an absence of mode-specific chemical effects. The results are also consistent with the notion that IVR is often not well described by a single exponential decay.[11,12]

The observed decoupling of sets of internal modes indicates that phase space is not explored ergodically on the time scale of the reactions, even at internal energies significantly greater than the dissociation thresholds. These results are consistent with and complementary to our earlier observation of trajectory rate coefficients that are considerably larger than corresponding statistical transition-state theory predictions computed on the same potential-energy surface.[1] It appears that the reactive trajectories find open reaction channels before a significant fraction of the energetically accessible phase space has been spanned. As a consequence, we find that mode-specific effects are present in the system. Trajectory rates are very sensitive to the nature of the initial energy partitioning and the isotope effects also show some evidence of mode-specific chemistry.

TABLE VIII. Effect of deuteration on total and branching microcanonical rate constants obtained from current trajectory calculations on Si_2X_6 where X = H,D. The ratio $k_D(E)/k_H(E)$ of the deuterated to the undeuterated rate constant is given for reaction channels with $k_H(E) \neq 0$.

	$k_D(E)/k_H(E)$				
E (eV)	$SiH_2 + SiH_4$	$SiH_3 + SiH_3$	$H_3SiSiH + H_2$	$Si_2H_5 + H$	Total
(a) Microcanonical energization					
5.31	0.79 ± 0.48	1.0 ± 1.1	1.2 ± 1.4	···	0.88 ± 0.43
6.31	0.76 ± 0.27	0.84 ± 0.30	0.48 ± 0.28	···	0.74 ± 0.18
7.31	0.96 ± 0.37	0.62 ± 0.17	0.59 ± 0.22	0.01 ± 0.13	0.65 ± 0.14
8.31	1.3 ± 0.9	0.79 ± 0.21	0.63 ± 0.35	0.65 ± 0.36	0.78 ± 0.19
9.31	2.5 ± 3.1	0.80 ± 0.17	0.95 ± 0.59	0.41 ± 0.36	0.81 ± 0.15
(b) Random energization					
5.31	0.69 ± 0.37	1.0 ± 1.1	0.71 ± 0.51	···	0.73 ± 0.29
6.31	0.74 ± 0.25	1.5 ± 0.6	0.67 ± 0.21	0.54 ± 0.59	0.83 ± 0.17
7.31	1.1 ± 0.5	1.1 ± 0.4	0.95 ± 0.31	0.37 ± 0.25	0.93 ± 0.23
8.31	1.1 ± 0.8	0.97 ± 0.32	0.52 ± 0.24	0.52 ± 0.30	0.71 ± 0.20
9.31	0.32 ± 0.38	0.91 ± 0.22	0.52 ± 0.28	0.54 ± 0.24	0.65 ± 0.12
(c) Local energization into Si–H (Si–D) modes					
5.31	1.5 ± 1.0	···	0.83 ± 0.43	0.98 ± 0.42	0.94 ± 0.32
6.31	1.8 ± 0.8	1.1 ± 0.7	0.69 ± 0.23	1.2 ± 0.4	1.06 ± 0.26
7.31	0.89 ± 0.32	1.3 ± 3.5	0.59 ± 0.69	0.93 ± 0.47	0.89 ± 0.41
8.31	···	···	0.47 ± 0.72	0.83 ± 0.18	0.80 ± 0.16
9.31	···	···	···	0.73 ± 0.10	0.74 ± 0.10
(d) Local energization into Si–Si modes					
5.31	···	0.53 ± 0.27	···	···	0.63 ± 0.30
6.31	···	0.64 ± 0.12	···	···	0.68 ± 0.13
7.31	···	0.74 ± 0.08	···	···	0.74 ± 0.08
8.31	···	0.76 ± 0.08	···	···	0.76 ± 0.07
9.31	···	0.81 ± 0.07	···	···	0.81 ± 0.07

ACKNOWLEDGMENTS

Thanks are due to Dr. Roland Kjellander of the University of Göteborg, Sweden, for the provision of a sophisticated plotting package (CURVES). Financial support from the Air Force Office of Scientific Research under Grant No. AFOSR-89-0085 is gratefully acknowledged.

[1]H. W. Schranz, L. M. Raff, and D. L. Thompson, J. Chem. Phys. **94**, 4219 (1991).
[2]H. W. Schranz, L. M. Raff, and D. L. Thompson, Chem. Phys. Lett. **171**, 68 (1990).
[3]P. M. Agrawal, D. L. Thompson, and L. M. Raff, J. Chem. Phys. **92**, 1069 (1990).
[4]J. D. Doll, J. Chem. Phys. **73**, 2760 (1980); **74**, 1074 (1984).
[5]W. H. Miller, J. Chem. Phys. **61**, 1622 (1974); **65**, 2216 (1976); B. C. Garrett and D. G. Truhlar, J. Phys. Chem. **83**, 1052 (1979); D. G. Truhlar and B. C. Garrett, Acc. Chem. Res. **13**, 440 (1980); P. Pechukas, Ann. Rev. Phys. Chem. **32**, 159 (1981).
[6]R. Viswanathan, D. L. Thompson, and L. M. Raff, J. Chem. Phys. **81**, 828 (1984); **81**, 3118 (1984); **82**, 3083 (1985).
[7]L. M. Raff, J. Chem. Phys. **90**, 6313 (1989).
[8]I. Oref and B. S. Rabinovitch, Acc. Chem. Res. **12**, 166 (1979).
[9]P. J. Robinson and K. A. Holbrook, *Unimolecular Reactions* (Wiley, New York, 1972).
[10]S. Nordholm and H. W. Schranz, Chem. Phys. **62**, 459 (1981); H. W. Schranz and S. Nordholm, *ibid.* **74**, 459 (1983).
[11]H. W. Schranz, PhD. thesis, University of Sydney, 1984.
[12]H. W. Schranz, S. Nordholm, and B. C. Freasier, Chem. Phys. **108**, 69, 93, 105 (1986).
[13]B. S. Rabinovitch and M. C. Flowers, Quart. Rev. **18** (1964) 122.
[14]H. W. Schranz and S. Nordholm, Chem. Phys. **87**, 163 (1984).
[15]J. D. Rynbrandt and B. S. Rabinovitch, J. Chem. Phys. **54**, 2275 (1971); J. Phys. Chem. **75**, 2164 (1971).
[16]P. J. Rogers, D. C. Montague, J. P. Frank, S. C. Tyler, and F. S. Rowland, Chem. Phys. Lett. **89**, 9 (1982); P. J. Rogers, J. I. Selco, and F. S. Rowland, *ibid.* **97**, 313 (1983); Y. Sakai, R. S. Iyer, and F. S. Rowland, J. Phys. Chem. **94**, 3368 (1990).
[17]S. P. Wrigley and B. S. Rabinovitch, Chem. Phys. Lett. **98**, 386 (1983), S. P. Wrigley, D. A. Oswald, and B. S. Rabinovitch, *ibid.* **104**, 521 (1984).
[18]K. E. Johnson, L. Wharton, and D. H. Levy, J. Chem. Phys. **69**, 2719 (1978); J. E. Kenny, D. V. Brumbaugh, and D. H. Levy, J. Chem. Phys. **71**, 4757 (1979).
[19]K. V. Reddy and M. J. Berry, Chem. Phys. Lett. **66**, 223 (1979).
[20]E. Thiele, M. F. Goodman, and J. Stone, Chem. Phys. Lett. **69**, 18 (1980); J. C. Stephenson, S. E. Biakowski, D. S. King, E. Thiele, J. Stone, and M. F. Goodman, J. Chem. Phys. **74**, 3905 (1981).
[21]P. Dietrich, M. Quack, and G. Seyfang, Chem. Phys. Lett. **167**, 535 (1990).
[22]R. E. Miller, Acc. Chem. Res. **23**, 10 (1990).
[23]E. W. Schlag and R. D. Levine, Chem. Phys. Lett. **163**, 523 (1989).
[24]J. Jortner and R. D. Levine, Isr. J. Chem. **30**, 207 (1990).
[25]V. Lopez and R. A. Marcus, Chem. Phys. Lett. **93**, 232 (1982); S. M. Lederman, V. López, V. Fairén, G. A. Voth, and R. A. Marcus, Chem. Phys. **139**, 171 (1989); T. Uzer and J. T. Hynes, *ibid.* **139**, 163 (1989), H. K. Shin, J. Chem. Phys. **91**, 929 (1989); *ibid* **92**, 5223 (1990).
[26]A. Vertes, R. Gijbels, and R. D. Levine, Rapid Comm. Mass. Spectrom. **4**, 228 (1990).
[27]T. A. Holme and R. D. Levine, Surf. Sci. **216**, 587 (1989).
[28]S. R. Vande Linde and W. L. Hase, J. Phys. Chem. **94**, (1990) 6148.
[29]S. H. Bauer and K. I. Lazaar, J. Chem. Phys. **79**, 2808 (1983); K. I. Lazaar and S. H. Bauer, J. Phys. Chem. **88**, 3052 (1984); S. H. Bauer,. Int. J. Chem. Kin. **17**, 367 (1985).
[30]D. B. Borchhardt and S. H. Bauer, J. Chem. Phys. **85**, 4980 (1983).
[31]S. H. Bauer, D. B. Borchhardt, and N.-S. Chiu, Ber. Bunsenges. Phys. Chem. **92**, 407 (1988).
[32]R. H. Newman-Evans, R. J. Simon, and B. K. Carpenter, J. Org. Chem. **55**, 695 (1990); also see J. Baggot, New Scientist January 6, 33 (1990).
[33]H. Gai and D. L. Thompson, Chem. Phys. Lett. **168**, 119 (1990).
[34]R. C. Baetzold and D. J. Wilson, J. Chem. Phys. **43**, 4299 (1965).
[35]D. L. Bunker and M. Pattengill, J. Chem. Phys. **48**, 772 (1968).
[36]D. L. Bunker and W. L. Hase, J. Chem. Phys. **59**, 4621 (1973); E. R. Grant and D. L. Bunker, *ibid.* **68**, 628 (1978).
[37]W. L. Hase, R. J. Wolf, and C. S. Sloane, J. Chem. Phys. **71**, 2911 (1979); R. J. Wolf and W. L. Hase, *ibid.* **72**, 316 (1980); **73**, 3779 (1980); **75**, 3809 (1981).
[38]C. C. Marston and N. De Leon, J. Chem. Phys. **91**, 3392 (1989); N. De Leon, *ibid.* **91**, 3405 (1989).
[39]S. Nordholm, Chem. Phys. **137**, 109 (1989).
[40]S. H. Courtney, M. W. Balk, L. A. Philips, S. P. Webb, D. Yang, D. H. Levy, and G. R. Fleming, J. Chem. Phys. **89**, 6697 (1988).
[41]B. A. Waite, S. K. Gray, and W. H. Miller, J. Chem. Phys. **78**, 259 (1983); S. Shi and W. H. Miller, Theor. Chim. Acta **68**, 1 (1985).
[42]E. L. Sibert, J. S. Hutchinson, J. T. Hynes, and W. P. Reinhardt, in *Ultrafast Phenomena IV*, edited by D. H. Auston and K. B. Eisenthal (Springer, New York, 1984); G. S. Ezra, in *Intramolecular and Nonlinear Dynamics*, edited by W. L. Hase (JAI, 1990).
[43]P. J. Nagy and W. L. Hase, Chem. Phys. Lett. **54**, 73 (1978).
[44]B. G. Sumpter and D. L. Thompson, J. Chem. Phys. **88**, 6889 (1988); H. Gai, D. L. Thompson, and G. A. Fisk, *ibid.* **90**, 7055 (1989); A. Preiskorn and D. L. Thompson, *ibid.* **91**, 2299 (1989); Y. Guan and D. L. Thompson, Chem. Phys. **139**, 147 (1989); J. Chem. Phys. **92**, 313 (1990).
[45]B. G. Sumpter and D. L. Thompson, J. Chem. Phys. **87**, 5809 (1987).
[46]L. M. Raff, J. Chem. Phys. **89**, 5680 (1988).
[47]W. P. Reinhardt and C. Duneczky, J. Chem. Soc. Faraday Trans. 2 **84**, 1511 (1988).
[48]T. A. Holme and R. D. Levine, Chem. Phys. **131**, 169 (1989).
[49]S. A. Rice and P. Gaspard, Isr. J. Chem. **30**, 23 (1990).
[50]M. Solc, Z. Phys. Chem. Neue Folge **166**, 103 (1989); D. L. Clarke and M. A. Collins, J. Chem. Phys. **92**, 5602 (1990).
[51]L. M. Raff and D. L. Thompson, in *Theory of Chemical Reaction Dynamics*, edited by M. Baer (Chemical Rubber, Boca Raton, 1985), Vol. III, p. 1.
[52]E. S. Severin, B. C. Freasier, N. D. Hamer, D. L. Jolly, and S. Nordholm, Chem. Phys. Lett. **57**, 117 (1978); E. S. Severin, Thesis BSc. Honours, University of New South Wales, R,. M. C. Duntroon, 1977.
[53]H. Hippler, H. W. Schranz, and J. Troe, J. Phys. Chem. **90**, 6158 (1986); H. W. Schranz and J. Troe, *ibid.* **90**, 6168 (1986).
[54]G. Nyman, K. Rynefors, and L. Holmlid, J. Chem. Phys. **88**, 3571 (1988); Chem. Phys. **125**, 171 (1989).
[55]H. W. Schranz, S. Nordholm, and G. Nyman, J. Chem. Phys. **94**, 1487 (1991).
[56]G. Nyman, S. Nordholm, and H. W. Schranz, J. Chem. Phys. **93**, 6767 (1990).
[57]W. H. Press, B. P. Flannery, S. A. Teukolsky, and W. T. Vetterling, *Numerical Recipes: The Art of Scientific Computing* (Cambridge University, Cambridge, 1988).
[58]K. A. Brownlee, *Statistical Theory and Methodology in Science and Engineering* (Wiley, New York, 1960).
[59]B. Efron, SIAM Rev. **21**, 460 (1979); P. Diaconis and B. Efron, Sci. Am. **248**, 96 (1983).
[60]E. B. Wilson, J. C. Decius, and P. C. Cross, *Molecular Vibrations* (McGraw-Hill, New York, 1955).